Escola de Primavera de Transição e Turbulência
Blumenau 2022

ABCM Associação Brasileira de Engenharia e Ciências Mecânicas

13th Spring School on Transition and Turbulence
September 19th-23rd, 2022, Blumenau, SC, Brazil

EPTT-2022-0027
RANDOM ERRORS IN HOT-WIRE ANEMOMETRY USING SYNTHETIC DATA

Livia S. Freire
Instituto de Ciências Matemáticas e de Computação, University of São Paulo, São Carlos, Brazil
liviafreire@usp.br

Abstract. *Hot-wire anemometers are one of the main tools used in the measurement of rapid velocity fluctuations in laboratory and natural flows. Their measurement frequency, which can reach the order of kilohertz, allows the investigation of turbulence fluctuations down to the smallest (dissipative) scales, providing a comprehensive description of turbulent flows. In this study, synthetic data that mimic hot-wire time-series velocity measurements are used to investigate random errors and their impact on turbulence statistics. The synthetic data are obtained from a prescribed three-dimensional energy spectrum, which includes the production, inertial and dissipation ranges, in addition to the bottleneck and intermittency effects, superposed by random errors typical of real data. The theoretical spectrum has a predefined Reynolds number, dissipation rate and mean streamwise velocity. From this spectrum, single-point time-series of the three velocity components are obtained from the inverse Fourier transform, assuming a homogeneous, isotropic and stationary flow. The probability distribution of turbulence statistics impacted by the random errors can be readily calculated from the synthetic time-series using the Monte-Carlo method. Examples of statistics include the dissipation rate estimated from energy spectra or second-order structure functions, providing useful information on error and bias. Finally, the method can serve several purposes, including educational training, code verification and validation, experiment planning, and testing and visualization of other types of measurement errors.*

Keywords: *Random erros, synthetic data, velocity time-series, turbulence*

1. INTRODUCTION

Due to its non-linear and chaotic nature, the study of turbulence relies on theories requiring validation or correction by experimental data. One classical example is the Kolmogorov's model for the inertial range of the energy spectrum. In brief, the concept of the energy cascade can be quantitatively described using three hypotheses: (i) that at sufficiently high Reynolds number, the small scales are isotropic (creating the local isotropy concept); (ii) that the smallest scales have a universal form uniquely determined by the fluid's kinematic viscosity ν and the turbulence kinetic energy (TKE) dissipation rate ε (defining the viscous scales, also known as the Kolmogorov scales, $\eta \equiv (\nu^3/\varepsilon)^{1/4}$, $u_\eta \equiv (\varepsilon\nu)^{1/4}$ and $\tau_\eta \equiv (\nu/\varepsilon)^{1/2}$ for length, velocity and time, respectively); and (iii) that the scales ℓ in the range $\ell_0 \gg \ell \gg \eta$ (where ℓ_0 is the largest scale of the flow) are uniquely determined by ε, independent of ν (Pope, 2000). As a result, the intermediate range of scales dominated by the energy cascade is characterized by a three-dimensional energy spectrum $E(\kappa)$ and second-order structure functions $D(r_1)$ in the form

$$E(\kappa) = C_k \varepsilon^{2/3} \kappa^{-5/3}, \tag{1}$$

$$D_{11}(r_1) = C_1 (\varepsilon r_1)^{2/3}, \tag{2}$$

$$D_{22}(r_1) = \frac{4}{3} C_1 (\varepsilon r_1)^{2/3}, \tag{3}$$

where D_{11} and D_{22} are the longitudinal and transversal structure functions, respectively, κ is the wavenumber corresponding to $2\pi/\ell$, r_1 is the longitudinal distance, and C_k and C_1 are empirical constants. The relevance of this model cannot be overstated. In addition to providing a signature of turbulence in a otherwise chaotic dataset, it also carries relevant information such as the TKE dissipation rate, which is typically difficult to measure directly. A drawback of the theory is the uncertainty on the empirical constants (Sreenivasan, 1995), in addition to the loose definition of "sufficiently high Reynolds number" (Antonia *et al.*, 2019), both of which have been extensively investigated but are still open for debate.

The investigation of this and many other turbulent theories require extensive measurements of different types of flows. In order to capture most, if not all, turbulence scales, hot-wire sensors have been widely used in both laboratory and field measurements (Vukoslavčević *et al.*, 1991; Saddoughi and Veeravalli, 1994; Metzger and Klewicki, 2001; Kang and Meneveau, 2006; Hutchins and Marusic, 2007; Metzger *et al.*, 2007; Folz and Wallace, 2010; Sinhuber *et al.*, 2017; Küchler *et al.*, 2019). Hot-wires are very fine wire sensors able to measure small-scale velocity fluctuations at frequencies

in the order of kilohertz. These anemometers are based on the concept of variation of the electrical resistance with temperature, through the use of a heated wire that senses the changes in heat transfer caused by fluctuations in the fluid velocity. Therefore, the output of the sensor is a time series of voltage that can be directly related to the time series of velocity fluctuations through the use of a calibration curve. One requirement for this method, however, is that the temperature, composition, and pressure of the fluid are constant, making the fluid velocity the only variable affecting the heat transfer (Lekakis, 1996). Although these conditions can usually be controlled in the laboratory, they are rarely met in the outdoor environment, which is a potential source of measurement errors. Furthermore, errors in calibration curve, low measurement frequency and many other possible sources of errors can impact the estimated turbulence parameters in ways that can be difficult to infer. Therefore, having a simplified tool that can help access errors and biases in this type of measurement can be useful in the interpretation of experimental data.

The impact of a Reynolds number that is not "sufficiently high" on turbulence statistics is also a potential source of error. Because the models for the inertial range (Eqs. (1)–(3)) are so simple, they are usually used isolated from the large (integral) and dissipative scales of the spectrum (or structure function). However, as discussed in details by Antonia *et al.* (2019), only at extremely large Reynolds numbers the Kolmogorov's hypotheses are valid, and a clear inertial range in experimental data may be difficult to obtain. To visualize the effect of a finite Reynolds number on the inertial range, a model spectrum such as the one proposed by Meyers and Meneveau (2008) can be used. In addition to the integral and dissipation ranges, this model includes the intermittency and bottleneck effects, which also impact the inertial range behavior. From the model spectrum, it is possible to generate synthetic single-point time-series data that possess the prescribed spectrum and, consequently, the corresponding second-order structure function. Furthermore, it is possible to include in the model spectrum random errors and any other artifact that mimics errors of real experimental data, and any statistics calculated from the synthetic time series (structure function, dissipation rate, etc.) can be compared to "the truth" (the prescribed values) in order to estimate the error and bias on each estimation (Freire *et al.*, 2019).

In this study, the model spectrum of Meyers and Meneveau (2008) is superposed to typical random errors present in measurements from hot-wire anemometers in order to investigate errors and biases in turbulence statistics extracted from measurement data. The methodology is presented here as a proof of concept, which can be easily extended to other types of problems. To exemplify, the impact of random errors on the estimation of the TKE dissipation rate is tested here. Other potential application are mentioned in the Conclusion section.

2. METHODS

2.1 Meyers and Meneveau (2008)'s model spectrum

The model spectrum proposed by Meyers and Meneveau (2008) is defined as

$$E(\kappa) = C_k \varepsilon^{2/3} \kappa^{-5/3} (\kappa L)^{-\beta} f_L(\kappa L) f_\eta(\kappa\eta), \tag{4}$$

$$f_L(\kappa L) = \left\{ \frac{\kappa L}{[(\kappa L)^p + \alpha_5]^{1/p}} \right\}^{5/3+\beta+2}, \tag{5}$$

$$f_\eta(\kappa\eta) = \exp(-\alpha_1 \kappa\eta) \left[1 + \frac{\alpha_2 (\kappa\eta/\alpha_4)^{\alpha_3})}{1 + (\kappa\eta/\alpha_4)^{\alpha_3}} \right], \tag{6}$$

in which L is the integral length scale, β is the intermittency correction for the inertial-range slope and f_L and f_η are non-dimensional functions representing the integral and dissipation scales, respectively. The main contributions from this approach compared to other models (such as Pope (2000)'s model spectrum) are the parameterization of the intermittency and bottleneck effects, the latter being the spectral bump at the transition between the inertial and dissipation scales, modeled by the term multiplying the exponential function in Eq. (6).

In addition to the flow scales L and η, related to the Reynolds number Re and TKE dissipation rate ε, the values of α_1–α_5 need to be prescribed in order to close the model. For a given Reynolds number, five flow constraints are used to obtain these constants, namely the total energy, enstrophy and palinstrophy from their corresponding integrals of the energy spectrum ($E(\kappa)$, $\kappa^2 E(\kappa)$ and $\kappa^4 E(\kappa)$, respectively), combined with the constraint for the height and location of the intermittency corrected dissipation peak (Eqs (6)-(8) and (11) of the original study). Therefore, the values of the Reynolds number, dissipation rate, and the derivative skewness (for the palinstrophy constraint) S_3 need to be chosen. In this study, the values of $Re_\lambda = 5900$ and 21180 were chosen from the atmospheric data measured by Tsuji (2004), which also provided the dissipation rate and mean streamwise velocity (needed for the Taylor's frozen turbulence hypothesis). Since it was not provided in the experiment, the value of $S_3 \approx -0.53$ was chosen (Sreenivasan and Antonia, 1997). The parameters $p = 1.5$ and $\beta = \mu/9$ (where $\mu = 0.25$ is the standard empirical value of intermittency exponent) were selected as in Meyers and Meneveau (2008). The Kolmogorov constant $C_k = 2.3$ was used as in the modeling of the same Tsuji (2004)'s data by Meyers and Meneveau (2008). Table 1 provides the model parameters for the present study, in which α_1–α_5 were obtained by solving their equations using the GNU Octave software (Eaton *et al.*, 2020).

From Meyers and Meneveau (2008)'s model, the following relations are used to obtain (numerically) the one-dimensional

Table 1. Parameters α_1–α_5 of the Meyers and Meneveau (2008)'s model estimated for Tsuji (2004)'s atmospheric data Re_λ, ε and $\overline{u}_1$. Measurement length and frequency used for the synthetic data generation.

Re_λ	5940	21180
$\overline{u}_1\,[\mathrm{m\,s^{-1}}]$	2.82	7.66
$\overline{\varepsilon}\,[\mathrm{m^2 s^{-3}}]$	0.0106	0.0760
α_1	5.01947	5.79054
α_2	2.90729	5.46142
α_3	2.17082	1.40221
α_4	0.13380	0.25055
α_5	5.79054	5.83688
measurement length (min)	30	15
measurement frequency (kHz)	2	4

energy spectra and second-order structure functions for each velocity component (Pope, 2000):

$$E_{11}(k_1) = \int_{k_1}^{\infty} \frac{E(\kappa)}{\kappa}\left(1 - \frac{k_1^2}{\kappa^2}\right) d\kappa, \tag{7}$$

$$E_{22}(k_1) = E_{33}(k_1) = \frac{1}{2}\left(E_{11}(k_1) - k_1 \frac{dE_{11}(k_1)}{dk_1}\right), \tag{8}$$

$$D_{\alpha\alpha}(r_1) = 2\int_0^{\infty} E_{\alpha\alpha}(k_1)[1 - \cos(k_1 r_1)]dk_1, \quad \alpha = 1, 2 \text{ or } 3, \tag{9}$$

in which k_1 is the longitudinal wavenumber. Equations (7) and (8) are only valid for locally homogeneous and isotropic flows (Hill, 1997); therefore, the model predictions presented here are only meaningful within the scales for which local isotropy is a reasonable assumption. Figure 1 shows the models for the two Re_λ cases tested here. Note that, in the typical log-log plot, the inertial range seems to cover several decades for both cases. In order to better visualize the errors in the inertial range, compensated functions in a linear-log plot will be presented in the Results section.

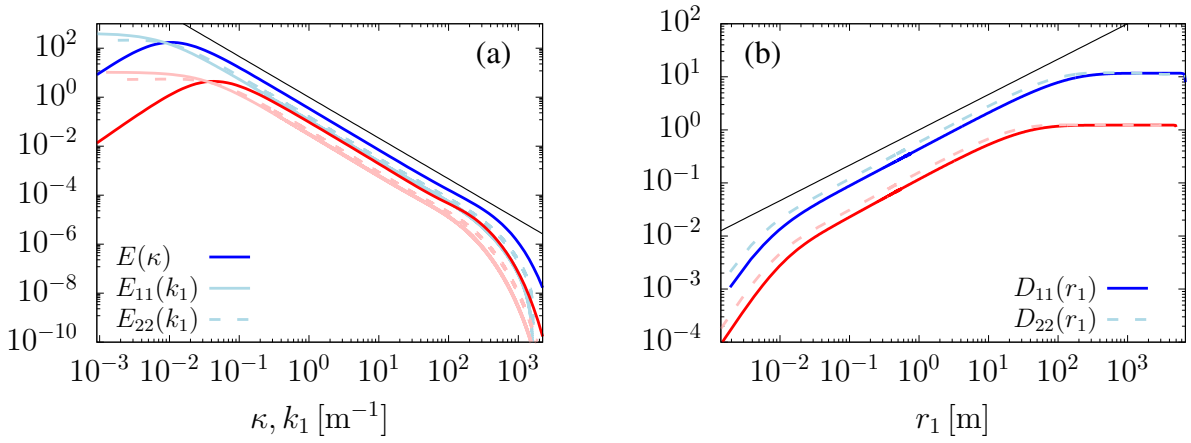

Figure 1. Meyers and Meneveau (2008)'s model for (a) three-dimensional energy spectrum ($E(\kappa)$), one-dimensional longitudinal ($E_{11}(k_1)$) and transversal ($E_{22}(k_1)$) spectra and (b) Longitudinal ($D_{11}(r_1)$) and transversal ($D_{22}(r_1)$) second-order structure functions. Red and blue lines correspond to $Re_\lambda = 21180$ and 5940, respectively. Black lines correspond to $\kappa^{-5/3}$ and $r_1^{2/3}$.

2.2 Synthetic time series

From a prescribed one-dimensional spectrum for each velocity component, a corresponding synthetic random velocity time-series is obtained as

$$u_i^s(t) = \mathrm{Re}\left\{\mathrm{FFT}\left\{[S_i(f)\Delta f]^{1/2}\sqrt{2}\exp(i\phi(f))\right\}\right\}, \tag{10}$$

where Re{ } denotes the real part of a complex number, FFT{ } is the fast Fourier transform, $S_i(f)$ is the desired spectral density of $u_i^s(t)$ as a function of the frequency f, Δf is the frequency increment and $\phi(f)$ is a random variable uniformly

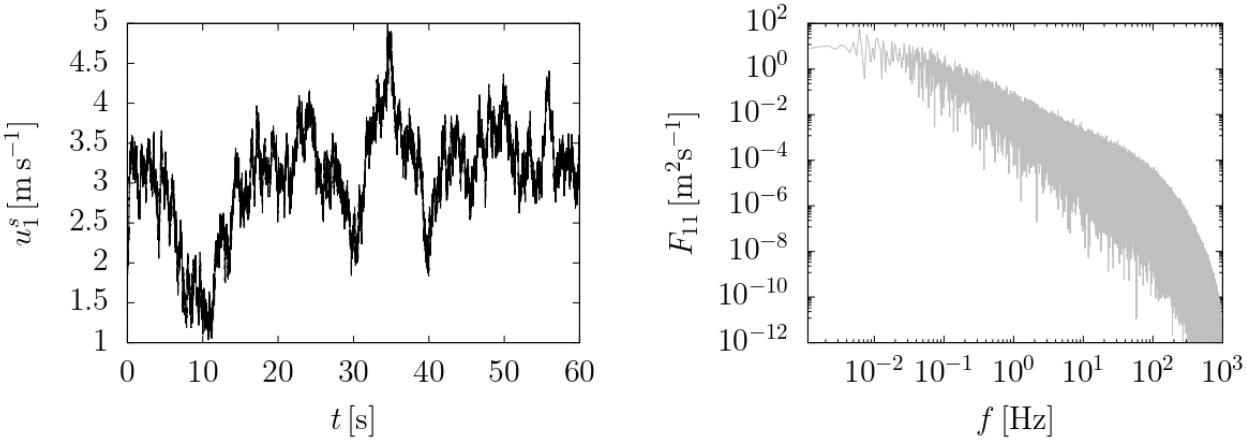

Figure 2. Example of synthetic time series $u_1^s(t)$ and its corresponding frequency spectrum $F_{11}(f)$.

distributed between zero and 2π, used to obtain independent random phase angles that create the velocity fluctuations in the time domain (Shinozuka and Deodatis, 1991). The result is a time series with spectral density exactly equal to $S_i(f)$ (except for numerical truncation). In order to evaluate the random errors of real hot-wire data, we define $S_i(f) = F_{\alpha\alpha}(f) + \sigma(f)y$, where $F_{\alpha\alpha} = E_{\alpha\alpha}(k_1)2\pi/\overline{u}_1$ (spectrum in the frequency domain from the spectrum in wavenumber domain using Taylor's frozen turbulence hypothesis, $\alpha = 1, 2$), $\overline{u}_1$ is the mean longitudinal velocity, $\sigma(f)$ is the standard deviation of a real spectrum and y is a random variable. As in Freire *et al.* (2019), we use the quasi-normal hypothesis and assume that the standard deviation of the spectrum is equal to its mean value, making $S_i(f) = F_{\alpha\alpha}(1 + y)$. In addition, $2(y + 1)$ follows a chi-square distribution with two degrees of freedom, making y a random variable with zero mean and variance equal to one. Figure 2 illustrates a synthetic time series and its corresponding frequency spectrum $F_{11}(f)$, which has the level of random error typically present in experimental data (Freire *et al.*, 2018, 2019).

3. RESULTS

As indicated in Fig. 2(b), the sample spectrum has a significant level of noise, requiring some averaging or smoothing when used in turbulence studies. The second-order structure function, on the other hand, is a smoother function by construction, since it corresponds to the integral of the spectrum (Eq. (9)). In a loose interpretation, we can say that, although both functions describe the energy held at different scales, in the case of the spectrum it shows the energy at the scale $\ell_1 = 2\pi/k_1$, while the structure function provides the energy of eddies with size r_1 or less (Davidson, 2004, p. 467), making the latter smoother. This difference is demonstrated by the average plus/minus one standard deviation of 1000 realizations, plotted in Fig. 3, and it is the reason that the structure function may be preferred over the spectrum in some inertial-range analyses. However, this same integral nature makes the length of the inertial range smaller in $D_{\alpha\alpha}(r_1)$ compared to $E_{\alpha\alpha}(k_1)$, which needs to be taken into account when interpreting this type of data, especially for lower Reynolds numbers. In the case of $Re_\lambda = 5940$, the inertial range of $D_{11}(r_1)$ is arguably absent (Fig. 3(c,d)).

The presence of the bottleneck effect, which is included in the model spectrum and can be seen in Fig. 3(a,b) (the bump in between the inertial and dissipation ranges), also impacts the length of the inertial range and potentially any information extracted from it. In the compensated structure function, its presence can be better seen for $Re_\lambda = 21180$ (at $r_1 \approx 0.02$), whereas for $Re_\lambda = 5940$ it is less clear, since the production range dominates the region where a flat profile should be present (if the Reynolds number were "sufficiently high").

Many tests regarding the impact of the random errors in the data can be performed. As a proof of concept, we show the estimation of the TKE dissipation rate ε from the fit of Kolmogorov's models (Eqs. (1) and (2)) to the inertial range of the sample spectrum and longitudinal structure function. This indirect estimate is typically performed when the measurement frequency is not high enough to capture all turbulence scales, a requirement in the estimation through the integral of the dissipation spectrum or using the velocity gradient. Figure 4 shows the probability density function (PDF) of dissipation, constructed from the 1000 realizations by matching Kolmogorov's models with the synthetic spectrum/structure function in the intervals $5 < k_1 < 10$ and $0.5 < r_1 < 1$, which is around the region where the inertial range is present (Fig. 3). The spread in ε values, due to the random error in the velocity time series, is larger for the spectrum than the structure function, as expected. Furthermore, there is a clear bias in all values obtained. The slightly positive bias in the spectrum case is likely related to the bottleneck effect, whereas the significant negative bias in the case of the structure function is probably caused by the finite Reynolds number effect, as it is more prominent for the lower Reynolds number. A more detailed evaluation, including the impact of the inertial range interval, Reynolds number, dissipation rate, mean velocity and many other parameters could be directly performed using the same approach.

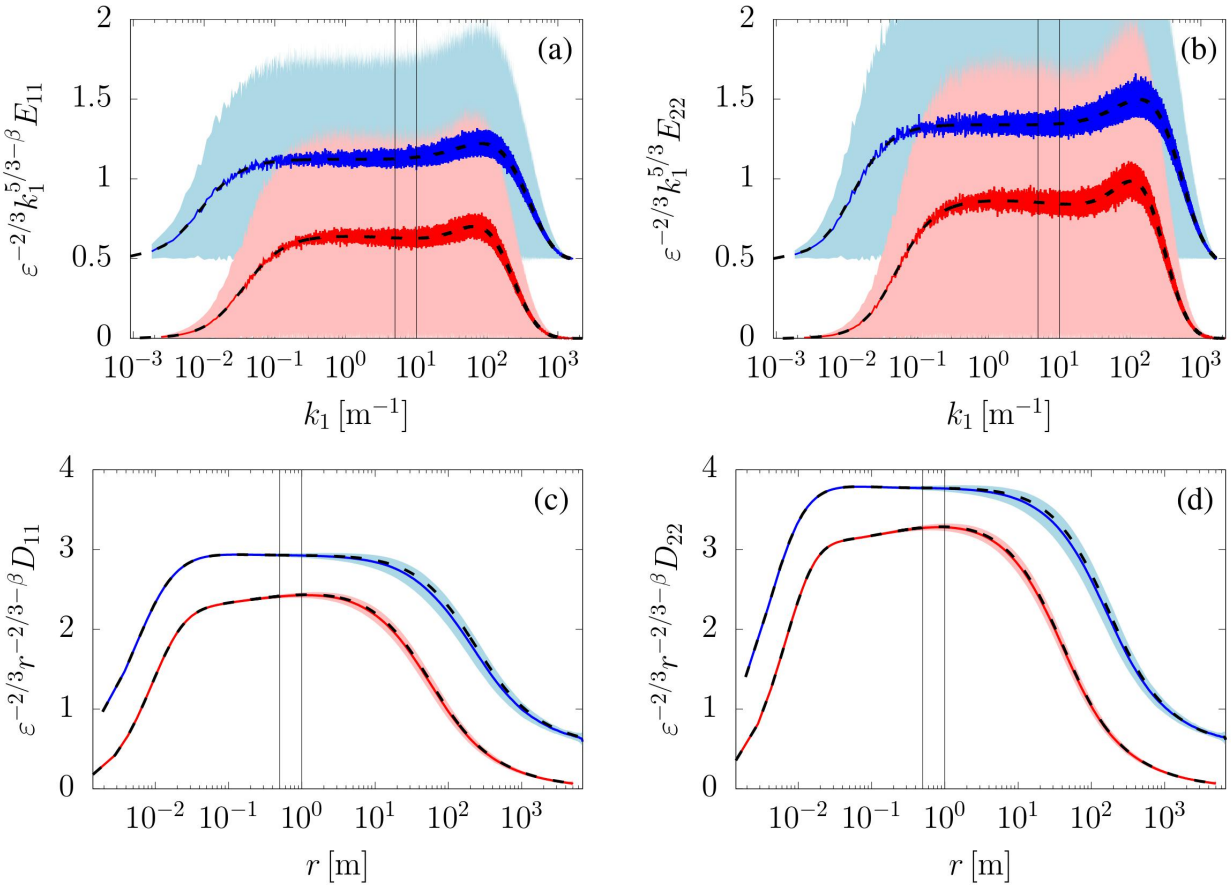

Figure 3. Average (dark colors) plus/minus one standard deviation (lighter shades) of the compensated one-dimensional spectra (a,b) and second-order structure functions (c,d) for $Re_\lambda = 21180$ (blue, shifted by 0.5) and 5940 (red). Black dashed lines correspond to the original models (Eqs. (7)–(9)). Vertical lines show the inertial range interval used for dissipation estimate.

4. CONCLUSION

This study provides a proof of concept on how to obtain random synthetic time series of single-point turbulent velocity measured by a hot-wire. The velocity data has a prescribed spectral density and the corresponding second-order structure function, in addition to an imposed Reynolds number and TKE dissipation rate. By introducing errors in the prescribed spectrum, such as random errors, path-averaging and aliasing effects, errors in the voltage-velocity calibration curve, and many others, it is possible to investigate their effect on many statistics typically extracted from this type of data. In addition, the tool can be used to test new methods of data analysis, as well as a learning tool on both turbulence theory and data processing. Finally, the tool can be used to generate synthetic data for code verification and validation, in addition to help in the planning of new experiments.

5. ACKNOWLEDGEMENTS

This study was funded by São Paulo Research Foundation (FAPESP, Brazil) Grants No. 2018/24284-1 and 2019/14371-7. The author acknowledges Marcelo Chamecki for insightful discussions.

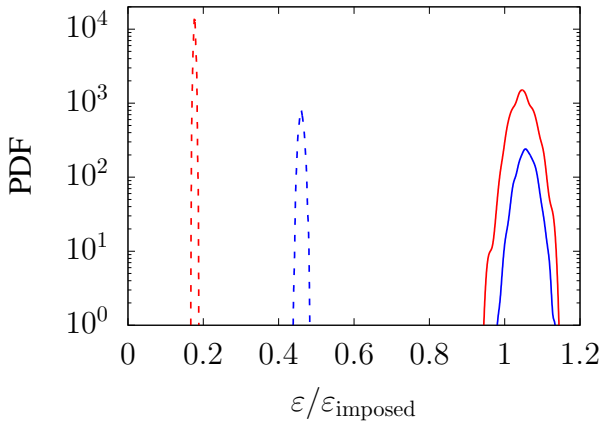

Figure 4. Probability density function of the estimated dissipation rate ε normalized by the imposed value. $Re_\lambda = 5940$ (red) and 21180 (blue), and estimates from the spectrum (solid) and second-order structure function (dashed lines).

6. REFERENCES

Antonia, R.A., Tang, S.L., Djenidi, L. and Zhou, Y., 2019. "Finite reynolds number effect and the 4/5 law". *Phys. Rev. Fluids*, Vol. 4, p. 084602. doi:10.1103/PhysRevFluids.4.084602.

Davidson, P., 2004. *Turbulence, an Introduction for scientists and engineerers*. Oxford University Press.

Eaton, J.W., Bateman, D., Hauberg, S. and Wehbring, R., 2020. *GNU Octave version 5.2.0 manual: a high-level interactive language for numerical computations*.

Folz, A. and Wallace, J.M., 2010. "Near-surface turbulence in the atmospheric boundary layer". *Physica D: Nonlinear Phenomena*, Vol. 239, No. 14, pp. 1305 – 1317. ISSN 0167-2789. doi:10.1016/j.physd.2009.06.014.

Freire, L.S., Dias, N.L. and Chamecki, M., 2019. "Effects of path averaging in a sonic anemometer on the estimation of turbulence-kinetic-energy dissipation rates". *Boundary-Layer Meteorology*, Vol. 173, pp. 99–113. ISSN 1573-1472. doi:10.1007/s10546-019-00453-4.

Freire, L.S., Dias, N.L. and Grion, A.L., 2018. "Uma comparação dos erros de estimativa da taxa de dissipação de energia cinética da turbulência por diferentes métodos na camada-limite atmosférica". *Ciência e Natura*, Vol. 40, pp. 7–13. doi:10.5902/2179460X30429.

Hill, R.J., 1997. "Applicability of Kolmogorov's and Monin's equations of turbulence". *Journal of Fluid Mechanics*, Vol. 353, pp. 67–81. doi:10.1017/S0022112097007362.

Hutchins, N. and Marusic, I., 2007. "Evidence of very long meandering features in the logarithmic region of turbulent boundary layers". *Journal of Fluid Mechanics*, Vol. 579, pp. 1–28. ISSN 1469-7645. doi:10.1017/S0022112006003946.

Kang, H.S. and Meneveau, C., 2006. "Experimental measurements of spectral subgrid-scale prandtl number in a heated turbulent wake flow, EDQNM predictions and 4/3-law". *Journal of Turbulence*, Vol. na, p. N45. doi:10.1080/14685240600622406.

Küchler, C., Bewley, G. and Bodenschatz, E., 2019. "Experimental study of the bottleneck in fully developed turbulence". *Journal of Statistical Physics*, Vol. 175, No. 3, pp. 617–639. ISSN 1572-9613.

Lekakis, I., 1996. "Calibration and signal interpretation for single and multiple hot-wire/hot-film probes". *Measurement Science and Technology*, Vol. 7, No. 10, pp. 1313–1333. doi:10.1088/0957-0233/7/10/004.

Metzger, M., McKeon, B. and Holmes, H., 2007. "The near-neutral atmospheric surface layer: turbulence and non-stationarity". *Philosophical Transactions of the Royal Society A: Mathematical, Physical and Engineering Sciences*, Vol. 365, No. 1852, pp. 859–876. doi:10.1098/rsta.2006.1946.

Metzger, M.M. and Klewicki, J.C., 2001. "A comparative study of near-wall turbulence in high and low reynolds number boundary layers". *Physics of Fluids*, Vol. 13, No. 3, pp. 692–701. doi:10.1063/1.1344894.

Meyers, J. and Meneveau, C., 2008. "A functional form for the energy spectrum parametrizing bottleneck and intermittency effects". *Physics of Fluids*, Vol. 20, No. 6, p. 065109. doi:10.1063/1.2936312.

Pope, S.B., 2000. *Turbulent Flows*. Cambridge University Press.

Saddoughi, S.G. and Veeravalli, S.V., 1994. "Local isotropy in turbulent boundary layers at high reynolds number". *Journal of Fluid Mechanics*, Vol. 268, p. 333–372. doi:10.1017/S0022112094001370.

Shinozuka, M. and Deodatis, G., 1991. "Simulation of stochastic processes by spectral representation". *Applied Mechanics Reviews*, Vol. 44, No. 4, pp. 191–204. ISSN 0003-6900. doi:10.1115/1.3119501.

Sinhuber, M., Bewley, G.P. and Bodenschatz, E., 2017. "Dissipative effects on inertial-range statistics at high reynolds

numbers". *Physical Review Letters*, Vol. 119, p. 134502. doi:10.1103/PhysRevLett.119.134502.

Sreenivasan, K.R. and Antonia, R.A., 1997. "The phenomenology of small-scale turbulence". *Annual Review of Fluid Mechanics*, Vol. 29, No. 1, pp. 435–472. doi:10.1146/annurev.fluid.29.1.435.

Sreenivasan, K.R., 1995. "On the universality of the kolmogorov constant". *Physics of Fluids*, Vol. 7, No. 11, pp. 2778–2784. doi:http://dx.doi.org/10.1063/1.868656.

Tsuji, Y., 2004. "Intermittency effect on energy spectrum in high-reynolds number turbulence". *Physics of Fluids*, Vol. 16, No. 5, pp. L43–L46. doi:10.1063/1.1689931.

Vukoslavčević, P., Wallace, J.M. and Balint, J.L., 1991. "The velocity and vorticity vector fields of a turbulent boundary layer. part 1. simultaneous measurement by hot-wire anemometry". *Journal of Fluid Mechanics*, Vol. 228, p. 25–51. doi:10.1017/S0022112091002628.

7. RESPONSIBILITY NOTICE

The author is the only responsible for the printed material included in this paper.